

BALANCING PROPERTIES OF CURRENT COMPARATOR CAPACITY-MEASURING NETWORK

By

E. SELÉNYI

Department of Instrumentation and Measurement, Technical University, Budapest

(Received September 3, 1968.)

Presented by Prof. Dr. I. SCHNELL

The development of high-quality magnetic materials — of low iron loss and of high permeability — has given the possibility to apply new electrical measuring methods.

The inductive measuring network, the precision current comparator developed in Canada in the first sixtieth makes it possible to measure current ratio at a high accuracy. Using current comparator — among others — the calibration of current transformer or the measurement of impedance can be achieved at a much higher accuracy than using any classical method.

The balancing properties of the network with current comparator suitable to measure capacity and loss factor will be analysed in this paper. When designing measuring networks with automatic balance, it is especially important to know the balancing properties.

The relations given in this publication are generally valid for the definite network: when plotting diagrams for demonstration, the actual circuit parameters (Chapter 5) of the measuring network with current comparator used in the C -tan δ Autorecorder developed at the Department of Instrumentation and Measurement of the Technical University were started of.

Finally, it has to be mentioned that this paper is discussing only the balance possibility among the measurement properties of the current comparator measuring network. So it does not deal with the synthesis of the network because to that purpose other measuring-technical aspects determined by the actual aim of the measurement have to be taken into account.

1. The layout of the measuring network

The circuit diagram of an impedance comparison bridge with current comparator is shown in Fig. 1, where

Z_x is the impedance to be measured,

Z_N is a high-accuracy normal impedance,

N_1 , N_2 and N_3 are the working and indicating windings of the current comparator,

U_g is the source of the measuring network.

In balanced state of the circuit the output voltage (U_{out}) equals zero, and so does the net excitation of the current comparator. As the ampere turns of windings N_1 and N_2 impair each other, the condition of compensation can be formulated as:

$$I_x N_1 = I_N N_2. \quad (1)$$

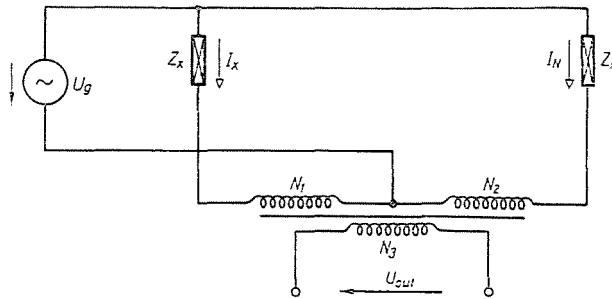


Fig. 1. Circuit for the comparison of impedances with current comparator

If upon balancing the voltage drop on the working windings is negligible (in general, the leakage inductive impedance and the resistance of copper are much lower than Z_x and Z_N), the balancing conditions are:

$$\frac{U_g}{Z_x} N_1 = \frac{U_g}{Z_N} N_2;$$

$$Z_x = Z_N \frac{N_1}{N_2}, \quad (2)$$

For analysing the network, the complex method of calculation for A. C. circuits is used, the source voltage (U_g) of the measuring mains taken as basic vector.

Relation (2) demonstrates the scheme in Fig. 1 to be only suitable for comparing equiphase impedances, in which case the measurement can be reduced to the determination of turn ratios.

To exactly measure simple impedances (the accomplished forms of elementary impedances — resistances, capacitances, inductances) the method should cover the measurement of the elementary impedance and its characteristic loss. Fig. 2 shows a network fitting to determine equivalent capacitance of series connection and its loss factor.

In balanced state the currents are:

$$I_x = j\omega C_x \frac{1}{1 + j\omega R_x C_x} U_g, \quad (3)$$

$$I_2 = j\omega C_N \frac{1}{1 + j\omega R(C + C_N)} U_g. \quad (4)$$

Taking into account Eq. (1) and the loss factor of the series equivalent connection ($\tan \delta_x = \omega R_x C_x$), the balancing condition is:

$$j\omega C_x N_1 \frac{1}{1 + j \tan \delta_x} U_g = j\omega C_N N_2 \frac{1}{1 + j\omega R(C + C_N)} U_g. \quad (5)$$

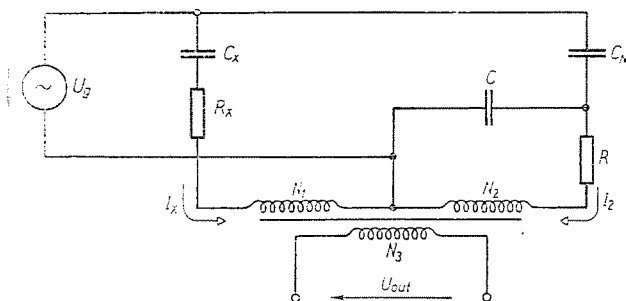


Fig. 2. Circuit for the measurement of capacitance

From Eq. (5) the unknown capacity and its loss factor can be determined as:

$$C_x = C_N \frac{N_2}{N_1}; \quad (6)$$

$$\tan \delta_x = \omega R(C + C_N). \quad (7)$$

The described capacitance-measuring network is used chiefly for measuring capacitance of high voltage industrial frequencies. Then the compensating elements of the connection are:

- N_1 — the setup capacity range,
- C — completed by C_N the setup range of $\tan \delta$,
- N_2 — balancing the capacitive component,
- R — balancing the loss factor.

In practice, balancing can be achieved by varying the balancing elements according to a suitable algorithm after setting up the adequate ranges, starting from any unbalanced state. The information needed to the variation is provided by the output signal.

Usual balancing algorithms are:

a) Minimum indication — minimation of the absolute value of the output signal in function of one parameter. After setting up the minimum, another balancing parameter is to be varied, again till the minimum absolute value of the output signal is reached. This process is to be repeated, till the output signal (error signal) will be small enough.

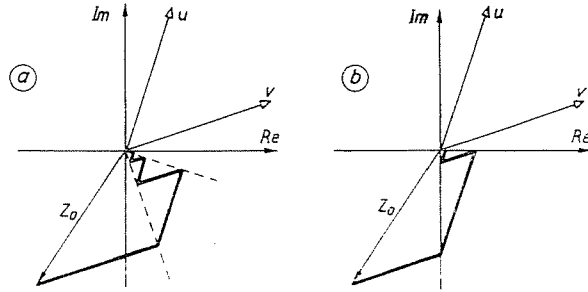


Fig. 3. Output signal change. a) with minimum indication. b) with phase-sensitive indication

b) Phase-sensitive indication — the output signal is decomposed into two normal components so that the value and direction of each component is characteristic for the detuning by each balancing parameter. Then varying one parameter should be done by zeroing the respective component in turn. In practice this balancing process means an iteration in several steps.

In Fig. 3 the output signal change, characteristic for the mentioned algorithms, is shown. The vectors u and v are pointing out the direction of the output signal change due to the balancing parameters, Z_0 is the initial error signal, the thick trace shows the migration of the end of the error vector in course of the balancing process.

2. Determination of output voltage

To estimate the balancing properties of the tested network requires to know the relationship between the output signal and the circuit parameters. Neglecting the leakage inductance and the copper resistance of the windings of the comparator, the measuring network shown in Fig. 4a can be transferred into the scheme shown in Fig. 4b. The relationship between the elements in a and b is given by the equations:

$$I'_x = U_g \frac{j\omega C_x}{1 + j \tan \delta_x} \frac{N_1}{N_3},$$

$$I'_2 = U_g \frac{j\omega C_N}{1 + j\omega R(C + C_N)} \frac{N_2}{N_3},$$

$$Y'_x = \frac{j\omega C_x}{1 + j \tan \delta_x} \frac{N_1^2}{N_3^2},$$

$$Y' = \frac{j\omega (C + C_N)}{1 + j\omega R(C + C_N)} \frac{N_2^2}{N_3^2},$$

$$Y_L = \frac{1}{j\omega \Lambda N_3^2}$$

Y_L is the admittance of the coil with N_3 turns, where Λ is the magnetic conductivity of the iron core,

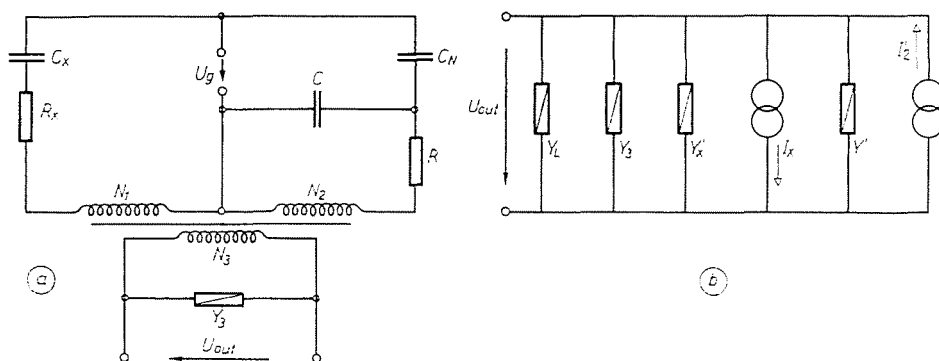


Fig. 4. a) Circuit for the measurement of capacitance. b) Equivalent circuit

Y_3 — admittance loading the indicating coil of the current comparator. On the basis of Fig. 4b the output voltage is:

$$U_{out} = \frac{U_g}{N_3} \left(\frac{j\omega C_N N_2}{1 + j\omega R(C + C_N)} - \frac{j\omega C_x N_1}{1 + j \tan \delta_x} \right) \frac{1}{Y_L + Y_3 + Y'_x + Y'}$$

Introducing the symbol $R(C + C_N) = \tan \delta_s$ ($\tan \delta$ set up) and neglecting Y'_x (the neglect is justified for usual circuit values, since here the condition $C_x N_1^2 \ll (C + C_N) N_2^2$ is usually satisfied) the output voltage is

$$U_{out} = U_g \left(\frac{j\omega C_N N_2}{1 + j \tan \delta_s} - \frac{j\omega C_x N_1}{1 + j \tan \delta_x} \right) \cdot \frac{j\omega \Lambda N_3 (1 + j \tan \delta_s)}{1 + j \tan \delta_s - \omega^2 (C + C_N) \Lambda N_2^2 + Y_3 j\omega \Lambda N_3^2 (1 + j \tan \delta_s)} \quad (8)$$

3. Properties of the measuring network near to the balanced state

Near the balanced state, a measuring network of zero-type alternating voltage can be characterized by the value and the phase-angle of the output signal (error signal) generated by each balancing parameter detuning. If, for a general case, Z is the complex output signal and u is a balancing parameter, then the sensitivity referred to u is:

$$S_u = \left| \frac{\partial Z}{\partial u} \right|_{Z=0}; \quad (9)$$

and the phase-angle of the direction of change:

$$\varphi_u = \arccos \frac{\partial Z}{\partial u} \Big|_{Z=0}. \quad (10)$$

Before applying Eqs (9) and (10) for the tested network, simplify the calculation by transforming Eq. (8):

$$U_{\text{out}} = K \cdot A,$$

where

$$K = N_2 \left(\frac{1 + j \tan \delta_x}{1 + j \tan \delta_s} \frac{C_N N_2}{C_x N_1} - 1 \right), \quad (11)$$

and

$$A = U_s \frac{-\omega^2 C_N A N_3}{1 + j \tan \delta_x - \omega^2 (C + C_N) A N_2^2 + Y_3 j \omega A N_3^2 (1 + j \tan \delta_x)}. \quad (12)$$

Eq. (12) has been written by introducing the equalities (6) and (7) referring to balanced cases. From the suitable form of the output signal (term K zeroed by balancing being of a simple structure) the balancing characteristics of the network are:

$$S_{N_2} = \left| \frac{\partial K}{\partial N_2} \cdot A \right|_{K=0} = |A|_{K=0}. \quad (13)$$

$$S_{\tan \delta_s} = \left| \frac{\partial K}{\partial \tan \delta_s} \cdot A \right|_{K=0} = \frac{N_2}{|1 + \tan^2 \delta_x|} |A|_{K=0}, \quad (14)$$

$$\varphi_{N_2} = \arccos \frac{\partial K}{\partial N_2} + \arccos A = \arccos A|_{K=0}, \quad (15)$$

$$\varphi_{\tan \delta_s} = \arccos \frac{\partial K}{\partial \tan \delta_s} + \arccos A = -\frac{\pi}{2} - \delta_x + \arccos A|_{K=0}. \quad (16)$$

In calculating the balancing characteristics — and also later — R was replaced by $\tan \delta_s = \omega R(C + C_N)$ differing from it by a constant factor alone. Eq. (13) through (16) involve both the absolute value and the phase angle of (12). The condition of the use of simple balancing algorithms is that vector A not greatly varies in function of the setup parameters. As it will be shown, this condition can be satisfied by adequate choice of Y_3 .

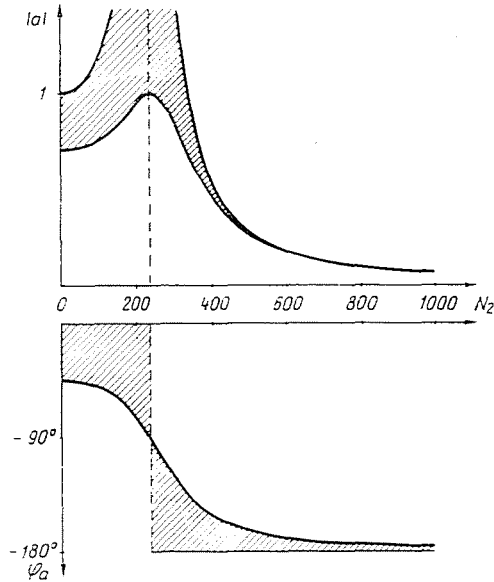


Fig. 5. Variation of the relative sensitivity-vector in the $\tan \delta$ range between 0 and 1

a) $Y_3 = 0$

In this case relationship (12) simplifies into:

$$A = U_g \frac{-\omega^2 C_N A N_3}{1 + j \tan \delta_x - \omega^2 (C + C_N) A N_2^2}$$

Introducing the relative sensitivity vector (from calculation aspects differing from A by a real factor only):

$$a = \frac{1}{1 + j \tan \delta_x - \omega^2 (C + C_N) A N_2^2}$$

and in the following, the variation of its absolute value and phase in function of N_2 and $\tan \delta_x$ for different $C + C_N$, i.e. $\tan \delta$ ranges will be examined.

Fig. 5 defines the amplitude and phase ranges of the relative sensitivity-vector as a function of N_2 , in the $\tan \delta$ range between 0 and 1 ($C + C_N = 3.18$

μF). The range is limited by traces for $\tan \delta = 0$ and $\tan \delta = 1$. Fig. 6 represents the relative sensitivity-vector in the $\tan \delta$ range from 0 to 0,1 ($C + C_N = = 318 \text{ nF}$).

From the figures the absolute value and the phase of the relative sensitivity-vector varying in wide ranges as function of the setup parameters can be seen. This means at the same time that sensitivities and directions of change

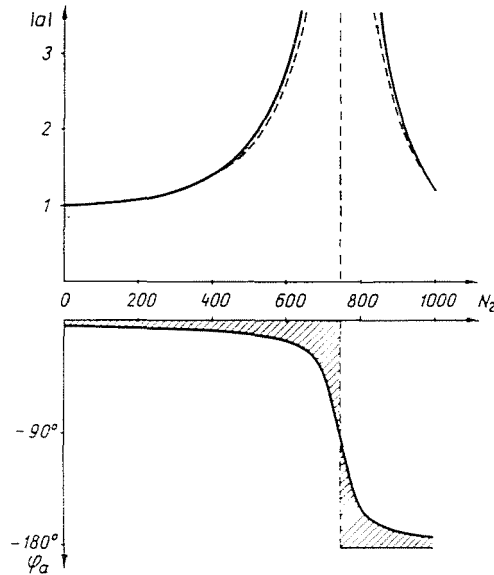


Fig. 6. Variation of the relative sensitivity-vector in the $\tan \delta$ range between 0 and 0,1

referred to the balancing parameters are strictly related to the object to be measured — i.e. on the balancing values of the scheme (See relationships (13) to (16). This fact makes more difficult the manual balancing and practically makes any of the automatic balancing by simple algorithms impossible. More “quietly” varying amplitude and phase of the relative sensitivity-vector is provided by a suitable choice of Y_3 .

$$b) Y_3 = j\omega C_3$$

Then, according to (12)

$$A = U_g \frac{-\omega^2 C_N A N_3}{(1 + j \tan \delta_x)(1 - \omega^2 C_3 A N_3^2) - \omega^2 (C + C_N) A N_2^2},$$

and the relative sensitivity vector:

$$a = \frac{1}{(1 + j \tan \delta_x)(1 - \omega^2 C_3 A N_3^2) - \omega^2 (C + C_N) A N_2^2}.$$

In Fig. 7 the stabilizing effect of various C_3 capacitances in $\tan \delta$ range from 0 to 1 is shown. The curves in Fig. 7a indicate the variation of the absolute value for $\tan \delta_x = 0$ in function of N_2 . (For $\tan \delta_x > 0$ the change of the amplitude is less, so it is less critical.) In Fig. 7b the curves of the phase varia-

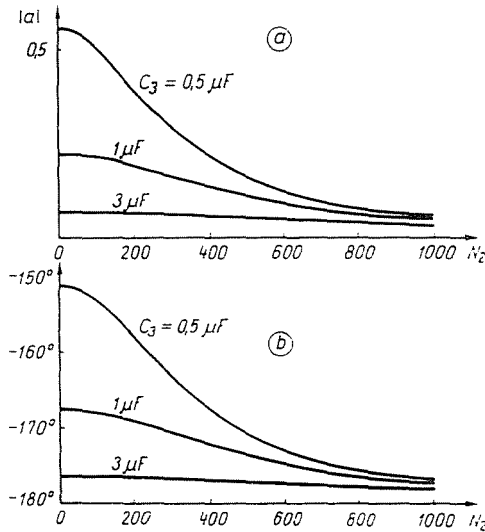


Fig. 7. Maximal variation of the relative sensitivity-vector with various C_3 ($\tan \delta$ range from 0 to 1)

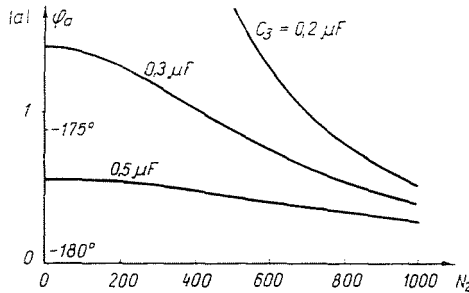


Fig. 8. Maximum variation of the relative sensitivity-vector with various C_3 ($\tan \delta$ range from 0 to 0.1)

tion refer to $\tan \delta_x = 1$. (For $\tan \delta_x < 1$ the phase variation is less.) Fig. 8 shows the influence of capacitance C_3 on the maximum amplitude and on the phase variation in $\tan \delta$ range from 0 to 0.1. Because of the small phase angles, the same curves suit to show amplitude and phase, applying different scales.

Figs 7 and 8 permit to determine C_3 values for different $\tan \delta$ ranges, pertaining to a given quality requirement. For instance, admitting a sensitivity decrease by 2 : 1 in function of N_2 , the capacity needed in the $\tan \delta$ range 0 to 1 is $\sim 3 \mu F$; in the $\tan \delta$ range 0 to 0,1 $\sim 0,5 \mu F$.

It can be seen that C_3 has a sensitivity-decreasing influence. Its linearizing character results from the fact that in case of a higher original sensitivity the decrease proportion is higher. To represent the sensitivity decrease, it is expedient to use the ratio of minima in the original and the linearized amplitude curves. For the C_3 values previously chosen ($3 \mu F$ and $0,5 \mu F$), this ratio is 2 or 3, that means that by using a twice or three times as sensible indicator, the same accuracy can be reached in the linearized network, as in the original one, which however, could hardly be balanced.

4. Behaviour of the measuring network far from the balance state

The examination near to the balance state does not describe fully the balancing properties of the network. Description of the network behaviour in case of big detunings requires to analyze the expression of the output voltage (8):

$$U_{\text{out}} = U_g \left(\frac{j\omega C_N N_2}{1 + j \tan \delta_s} - \frac{j\omega C_x}{1 + j \tan \delta_x} \right) \cdot \frac{1}{(1 + j \tan \delta_s)(1 + Y_3 j\omega A N_3^2) - \omega^2 (C + C_N) A N_2^2}$$

The terms in the relationship can be classified as:

a) Terms describing the measurement:

$$C_x; \tan \delta_x; U_g; \omega$$

b) Construction data of the network:

$$N_3; A$$

c) Setup data of the network:

$$N_1; C_N; C + C_N; Y_3$$

d) Balancing parameters:

$$N_2; \tan \delta_s$$

It has to be pointed out that for big detunings, A (magnetic conductivity of the iron core) is not more a real and constant value because of the non-linearity and loss of iron, but depends on the induction and thus on the output voltage:

$$A = f(|U_{\text{out}}|), \quad (\text{see Fig. 14})$$

In the following the output voltage will be analysed in function of the balancing parameters, for fixed data in groups $a-b-c$. For illustrating the balancing

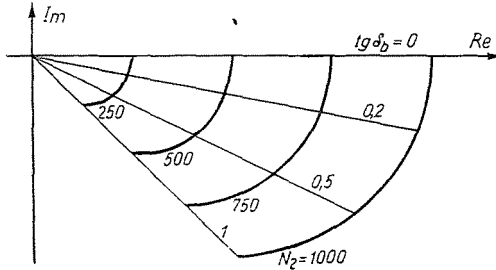


Fig. 9. The theoretical balancing trajectory

properties the balancing trajectories of the scheme are used. The balancing trajectory shows the variation of the output voltage in the complex system of numbers. It consists of two sets of curves:

$$\begin{aligned} U_{\text{out}} &= f(N_{2i}; \tan \delta_{si}) & 0 \leq N_2 \leq N_{2\text{max}} & \quad i = 1, 2, \dots, n, \\ U_{\text{out}} &= f(N_{2j}; \tan \delta_s) & 0 \leq \tan \delta_s \leq \tan \delta_{s\text{max}} & \quad j = 1, 2, \dots, m. \end{aligned}$$

a) The theoretical balancing trajectory of the measuring network

The theoretical balancing trajectory is based on the following assumptions:

- the voltage drops on the coils of the comparator can be neglected,
- the iron core of the comparator is free of losses and has a linear magnetization curve, furthermore $Y_3 = 0$.

According to Eqs (3) and (4), with these assumptions the net excitation is:

$$\Theta = U_g \left(\frac{j\omega C_N N_2}{1 + j \tan \delta_s} - \frac{j\omega C_x N_1}{1 + j \tan \delta_x} \right),$$

and the output voltage:

$$U_{\text{out}} = j\omega N_3 A \Theta = j\omega N_3 A U_g \left(\frac{j\omega C_N N_2}{1 + j \tan \delta_s} - \frac{j\omega C_x N_1}{1 + j \tan \delta_x} \right). \quad (17)$$

The character of the balancing trajectory described by the relationship (17) is shown in Fig. 9. (In the figure the trajectory $-U_{\text{out}}$ is presented, because

it is more suitable for further comparisons.) By appropriately shifting the zero point of the coordinate system, the trajectories belonging to various C_x and $\tan \delta_x$ values can be obtained. In Fig. 10a there is shown the balancing adjustment based on minimum indication, and in Fig. 10b the balancing adjustment based on phase-sensitive indication. In both figures the variation of the output voltage is traced by thick line.

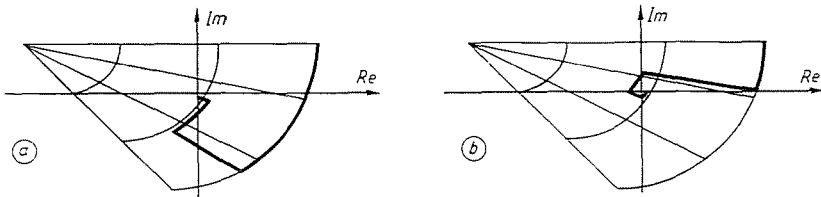


Fig. 10. The balancing adjustment. a) with minimum indication, b) with phase-sensitive indication

b) Real balancing trajectories of the measuring network

In the following, balancing trajectories belonging to some setups of the capacitance-measuring network with current comparator are given. The setup specifications belonging to several figures are given in Table 1.

Table 1

Setup specifications for figures 11 to 13

| Fig. | U_g | C_x | $\tan \delta_x$ | C_c |
|------|--------|-------|-----------------|-----------|
| 11a. | 10kV | 3 nF | 0 | 0 |
| 11b. | 100 kV | 3 nF | 0 | 0 |
| 11c. | 100 kV | 3 nF | 0 | 3 μF |
| 11d. | 100 kV | 3 nF | 0 | 1 μF |
| 12a. | 10 kV | 3 nF | 1 | 0 |
| 12b. | 100 kV | 3 nF | 1 | 0 |
| 12c. | 100 kV | 3 nF | 1 | 3 μF |
| 13a. | 10 kV | 8 nF | 0 | 0 |
| 13b. | 100 kV | 8 nF | 0 | 0 |
| 13c. | 100 kV | 8 nF | 0 | 3 μF |

$$C_N = 100 \text{ pF}$$

$$N_1 = 10 \text{ turns}$$

$$C + C_N = 3,18 \text{ } \mu F$$

Conclusions from the balancing trajectories:

1. All the figures marked "a" are characterized by a source voltage of 10 kV and by the absence of any linearizing C_3 . In these conditions the core of the comparator works on the beginning, quasi-linear section of the magnetization curve, (it means too, that trajectories of a source voltage below 10 kV will be similar to the presented ones). From the figures the high degree of

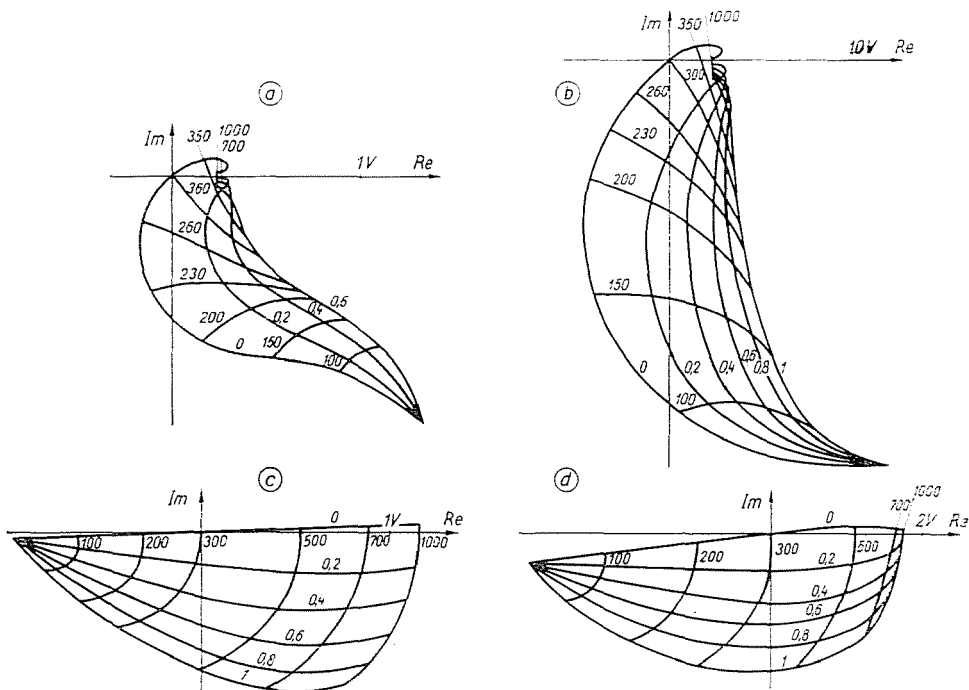


Fig. 11. Balancing trajectories (see Table. 1)

curvature of the trajectories appears, which is caused by amplitude — and phase — variation of the relative sensitivity vector analyzed before. Notice that none of the described simple balancing algorithms is suitable to achieve balance from an arbitrary unbalanced state. It is exceedingly striking how amplitude-minimizing algorithms are useless in ranges of great number of turns — $500 < N_2$ — for the trajectories in 11a and 12a.

2. In figures marked "b" the source voltage is 100 kV and the linearizing C_3 is absent again. The difference between trajectories *b* and the corresponding *a* ones is caused by the non-linearity of the comparator core.

For the current comparator used in the measuring network (Chapter 5) the next statement is approximately valid: in case of identical phase of excitation the output voltage $4-24V$ ($0,1 \text{ Tesla} < B < 0,6 \text{ Tesla}$) has a phase lag against the output voltage in quasi-linear range $0-4V$ ($0 < B < 0,1 \text{ T}$):

the output voltage in the range 24–30 V ($0,6T < B < 0,75 T$) has a phase lead. (At 30 V the comparator is practically saturated.)

These facts mean that the under 4 V range of figures "b" are similar to the ones of figures a; their parts between 4 and 24 V have a lag and over 24 V have a lead in comparison to the corresponding a.

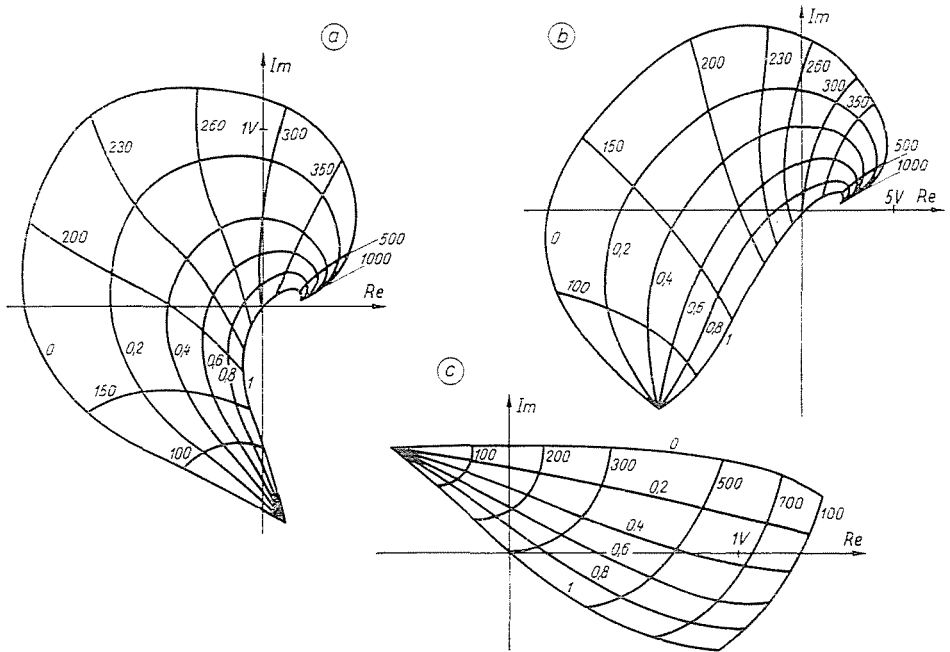


Fig. 12. Balancing trajectories (see Table 1)

The saturating character of the iron core results in a further distortion of the trajectories (Fig. 13b), which is further impairing the balancing possibility.

3. In the figures c the linearizing effect of capacitance $C_3 = 3 \mu F$ for a source voltage of 100 kV is shown. The trajectories diverge but slightly from the theoretical ones of measuring network with current comparator (Fig. 9). As it can be seen, linearizing can be reached at the expense of an output voltage decrease by about one order. This is, however, unimportant in case of big detunings, while near to the balance the conditions explained there are valid.

4. In Fig. 11d the influence of a smaller ($C_3 = 1 \mu F$) linearizing capacitance is shown. For great numbers of turn the trajectory is seen to be distorted. Though, principally, the balance can be reached by any of the algorithms, in practice it will be more difficult to balance from the distorted range because of adjustment errors of the minima i.e. of the component 0 points.

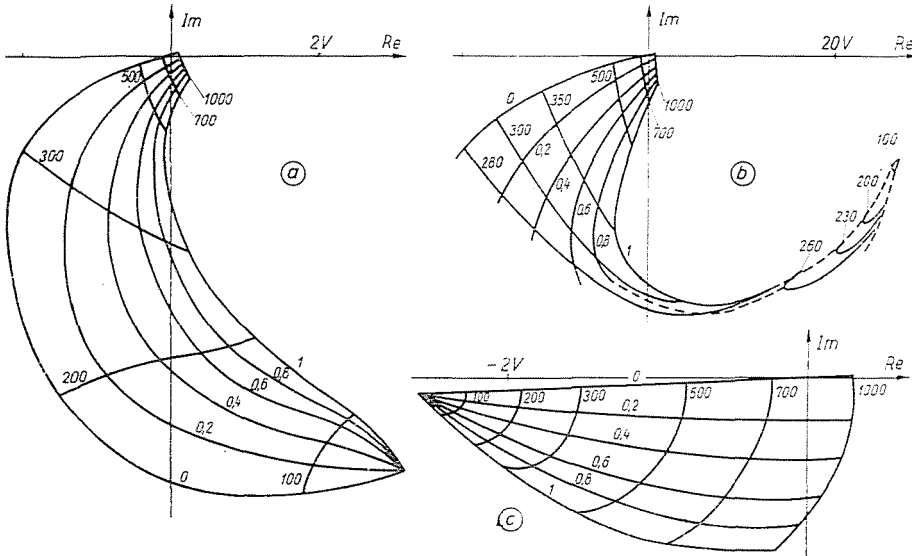


Fig. 13. Balancing trajectories (see Table 1)

5. Data of the measuring network

the calculation is based on

a) Data characteristic for the measurement:

| | |
|-----------------|--|
| C_x | ranges from $10 C_N$ to $10^4 C_N$ in four steps |
| $\tan \delta_N$ | ranges from 10^{-2} to 1 in seven steps |
| U_g | its maximum depends on C_N |
| f | 50 Hz |

b) Construction data of the measuring network:

| | |
|--|---------------------|
| N_3 | 1000 turns |
| geometric data of the thoroid iron core: | |
| — iron cross-section | 1,9 cm ² |
| — average length of the force lines | 35 cm |
| — magnetic properties | — see Fig. 14 |

c) Setup data of the measuring network:

| | |
|-----------|--|
| N_1 | from 0,1 to 100 turns in four ranges |
| C_N | max 1 nF |
| $C + C_N$ | 31,8 nF — 3,18 μ F in seven ranges |

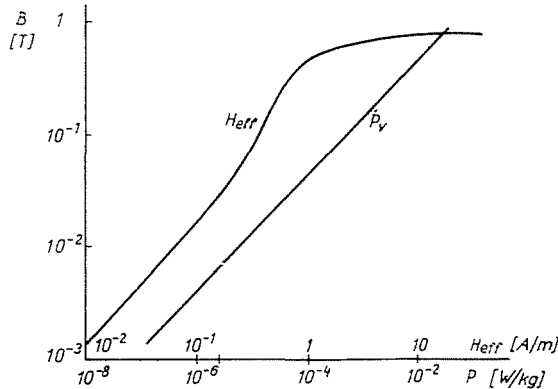


Fig. 14. Magnetic properties of the thoroid iron core of the current comparator

d) Balancing parameters:

| | |
|-------|----------------|
| N_2 | 0 — 1000 turns |
| R | 0 — 1000 ohms |

Summary

This paper describes the analysis of the balancing properties of a capacitance measuring network with current comparator. The method — determination of sensitivities and balancing directions near to the balance, representation of the output signal change caused by big detunings in form of trajectories — is generally suitable to obtain the balancing properties of alternative-current 0-method measuring networks (e.g.: impedometric bridges).

The analysis is stated to be based on the determination of the output signal function. Determination of the output voltage for the given network involves general steps and neglects helpful in the analysis of other current comparator measuring networks.

References

1. KUSTERS, N. L.—MOORE, W. J. M.: The Current Comparator and Its Application to the Absolute Calibration of Current Transformers. *Trans. AIEE (Power Apparatus and Systems)*, **80**, 94—104. (1961).
2. MILJANIC, P. N.—KUSTERS, N. L.—MOORE, W. J. M.: The Development of the Current Comparator, a High-accuracy A—C Ratio Measuring Device. *Trans. AIEE (Commun. and Electronics)*, **81**, 359—368. (1962).
3. KUSTERS, N. L.—PETERSONS, O.: A Transformer-Ratio-Arm Bridge for High-Voltage Capacitance Measurements. *IEEE Trans. on Commun. and Electronics*, 606—611, (1963).
4. CALVERT, R.—MILDWATER, J.: Self-Balancing Transformer Ratio Arm Bridges. *Electronic Eng.* **35**, 782—787 (1963).
5. PETERSONS, O.: A Self-Balancing High-Voltage Capacitance Bridge. *IEEE Trans. on Instrumentation and Measurement*, **IM-13**, 216—224, (1964).
6. PETERSONS, O.: A Self-Balancing Current Comparator. *IEEE Trans. on Instrumentation and Measurement*, **IM-15**, 62—71 (1966).
7. LEVIN, M. J.: The Sensitivity of Transformer Measuring Bridges. *Avtometriya No. 3*, 75—82 (1967). In Russian.

Endre SELÉNYI, Budapest XI., Műegyetem rkp. 9, Hungary.